

This document is confidential and is proprietary to the American Chemical Society and its authors. Do not copy or disclose without written permission. If you have received this item in error, notify the sender and delete all copies.

pH-Triggered Reversible Multiple Protein-Polymer Conjugation based on Molecular Recognition

Journal:	<i>The Journal of Physical Chemistry</i>
Manuscript ID:	jp-2015-066375.R1
Manuscript Type:	Article
Date Submitted by the Author:	07-Aug-2015
Complete List of Authors:	Liu, Juan; University of Basel, Department of Chemistry Postupalenko, Viktoriia; University of Basel, Department of Chemistry Duskey, Jason; University of Basel, Department of Chemistry Palivan, Cornelia; University of Basel, Chemistry Department Meier, Wolfgang; University of Basel, Department of Chemistry

SCHOLARONE™
Manuscripts

1
2
3
4
5
6
7
8
9
10
11
12
13
14
15
16
17
18
19
20
21
22
23
24
25
26
27
28
29
30
31
32
33
34
35
36
37
38
39
40
41
42
43
44
45
46
47
48
49
50
51
52
53
54
55
56
57
58
59
60

pH-Triggered Reversible Multiple Protein-Polymer Conjugation based on Molecular Recognition

Juan Liu, Viktoriia Postupalenko, Jason T. Duskey, Cornelia G. Palivan, Wolfgang Meier**

Department of Chemistry, University of Basel, Klingelbergstrasse 80, Basel 4056, Switzerland

1
2
3 **ABSTRACT:** Polymer conjugation for protein based therapeutics has been developed
4 extensively; but still suffers from conjugation leading to decrease in protein activity, and
5 generates complexes with limited diversity due to general classical systems only incorporating
6 one protein per each complex. Here we introduce a site specific non-covalent protein-polymer
7 conjugation, which can reduce the heterogeneity of the conjugates without disrupting protein
8 function, while allowing for the modulation of binding affinity and stability, affecting the pH
9 dependent binding of the number of proteins per polymer. We compared classical one protein
10 polymer conjugates with multiple protein polymer conjugates using His-tagged enhanced yellow
11 fluorescence protein (His₆-eYFP) and metal-coordinated tris-nitrilotriacetic acid (trisNTA-Meⁿ⁺)
12 in a site-specific way. trisNTA-Meⁿ⁺-His₆ acts as a reversible linker with pH triggered release of
13 functional protein from the trisNTA functionalized copolymers. The nature of the selected Meⁿ⁺
14 and number of available trisNTA-Meⁿ⁺ on poly(N-isopropylacrylamide-*co*-tris-nitrilotriacetic
15 acid acrylamide) (PNT) copolymers enable predictable modulation of the conjugates binding
16 affinity (0.09-1.35 μM), stability, cell toxicity, and pH responsiveness. This represents a
17 promising platform that allows direct control over the properties of multiple protein polymer
18 conjugates compared to the classical single protein polymer conjugates.
19
20
21
22
23
24
25
26
27
28
29
30
31
32
33
34
35
36
37
38
39
40
41
42
43
44
45
46
47
48
49
50
51
52
53
54
55
56
57
58
59
60

INTRODUCTION

Protein therapeutics is of high importance in almost every field of medicine.¹ However, there are still a number of challenges in the application of protein therapeutics that have to be overcome.^{1,2}

Therapeutic proteins exhibit low stability, fast renal clearance, enzymatic degradation, and are frequently immunogenic.³

An elegant way to overcome these problems is to conjugate polymers to proteins, which has been reported to improve protein stability, half-life, solubility, and reduce immunogenicity.⁴⁻⁸

However, such conjugation can lead to the alteration of the protein structure, resulting in a decrease or even complete inhibition of protein activity.^{9,10} An effective approach to overcome a loss of protein function is to design stimuli-responsive linkage between polymers and proteins.¹¹

This enables the linkage to be independent of the protein function, and therefore, cleavage of the protein from the polymer conjugate by a specific stimulus releases the intact and functional protein.¹¹⁻¹³ Currently, covalent attachment of polymers to proteins through stimuli-cleavable

linkers has mainly been developed.^{11,13-15} Non-covalent interactions with a stimuli-responsive nature are rarely applied for protein-polymer conjugation due to their instability.^{16,17} The interaction between metal-coordinated nitrilotriacetic acid (NTA-Meⁿ⁺) and His-tagged proteins is a promising candidate for protein-polymer conjugation, due to the binding specificity and the reversibility upon pH change or the addition of imidazole or ethylenediaminetetraacetic acid (EDTA).^{18,19} Also, no modification of the protein is required as most recombinant therapeutic

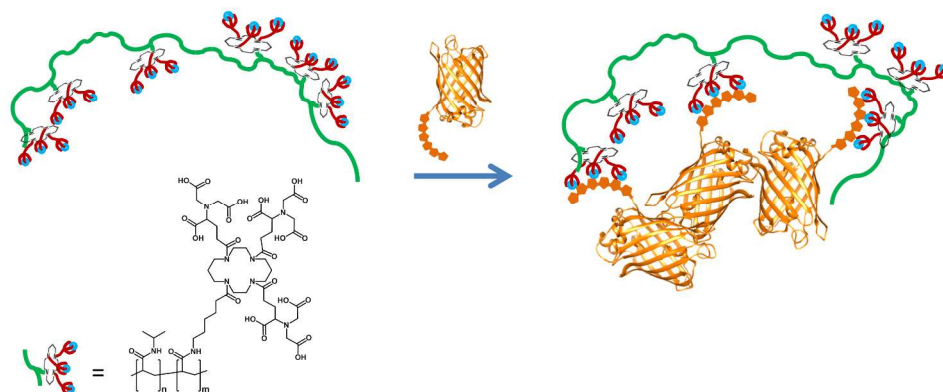
proteins expressed by E.coli incorporate his tag (His₆) for affinity purification, which can also directly coordinate the NTA-Meⁿ⁺. Unfortunately, to the best of our knowledge, there is only one study published using NTA-Meⁿ⁺-His₆ for the formation of protein-polymer conjugates for protein therapy, but the conjugates were shown to exhibit low stability due to the poor binding

1
2
3 affinity.¹⁶ Supramolecular entities with two or three NTA heads (bisNTA and trisNTA,
4 respectively) exhibit improved binding affinity towards His-tagged proteins, and have been used
5 recently for the formation of protein-polymer conjugates.^{16,20} Among them, trisNTA possesses
6 the highest binding affinity,^{19,21-24} but the stability and the pH-triggered releaseability of trisNTA-
7 Me²⁺-His₆ protein-polymer conjugates is still unknown.

8
9
10 Moreover, most protein-polymer conjugate systems allow for only one protein to be bound to
11 each or multiple polymers.^{7,25} Binding multiple proteins on each polymer would be able to
12 enhance the stability of conjugates due to the inter-protein interactions, similar to many natural
13 stabilized protein assemblies.²⁶⁻²⁸

14
15 A previous study published by our group introduced poly(N-isopropylacrylamide-*co*-tris-
16 nitrilotriacetic acid acrylamide) copolymers (PNTn, where n represents the mol% of trisNTA on
17 the polymer) containing Cu²⁺ for specific binding of His-tagged molecules.²⁰ Here, we employ
18 PNTn copolymers and His₆-eYFP (Figure 1) as models for polymer-protein conjugation to
19 analyze the effect on the stability, pH-triggered dissociation, and toxicity when variables such as
20 the nature of the metal, the distance between trisNTA sites, and the addition of inter-protein
21 interactions were varied. Three metal cations, Cu²⁺, Zn²⁺, and Fe³⁺, were chosen as the
22 coordination center in the trisNTA pocket to modulate the binding affinity of His-tagged proteins
23 to the polymer, and were assessed by isothermal titration calorimetry (ITC). Then their ability to
24 reversibly bind based on changes in pH was analyzed by fast protein liquid chromatography
25 (FPLC). Also, the protein stability before and after conjugation, as well as after pH mediated
26 release, were measured by circular dichroism (CD) and fluorescence spectroscopy. Our strategy
27 of multiple protein conjugation to each polymer chain, and release upon pH changes can be
28
29
30
31
32
33
34
35
36
37
38
39
40
41
42
43
44
45
46
47
48
49
50
51
52
53
54
55
56
57
58
59
60

1
2
3 expanded to other systems, and advance the application of non-covalent interactions for protein-
4
5 polymer conjugation.
6
7
8
9



35
36
37
38
39
40
41
42
43
44
45
46
47
48
49
50
51
52
53
54
55
56
57
58
59
60

Figure 1. Schematic representation of site-specific conjugation of poly(N-isopropylacrylamide-*co*-tris-nitrilotriacetic acid acrylamide) polymers (green), which coordinate metals (blue) with His-tagged proteins (orange).

EXPERIMENTAL SECTION

Materials. Copper(II) chloride, zinc chloride, iron(III) sulfate hydrate, Dulbecco's modified eagle medium (DMEM) and phosphate buffered saline (PBS) were purchased from Sigma-Aldrich and used as received. 3-(4,5-dimethylthiazol-2-yl)-5-(3-carboxymethoxyphenyl)-2-(4-sulfophenyl)-2H-tetrazolium (MTS) was purchased from Promega, USA. Penicillin, streptomycin and fetal bovine serum (FBS) were purchased from Life technologies. Rhodamine B labelled hexahistidine (RHB-His₆) was received as a gift from Dr. Thomas Schuster. PierceTM BCA Protein Assay was from Thermo Scientific. All chemicals were purchased with the highest purity and used without further purification unless otherwise stated.

1
2
3 **Chelation of metal cations to PNTn copolymers.** Respective PNTn (0.2 mg/mL) were
4 dissolved in PBS, pH 7.4. A stoichiometric excess of CuCl_2 , ZnCl_2 , or $\text{Fe}_2(\text{SO}_4)_3$ was mixed with
5 the respective PNTn solution and was purified on a HiTrap desalting column (5 mL, GE
6 Healthcare Life Sciences) with PBS as the mobile phase.
7
8
9

10
11 **Protein expression and analysis.** The expression of His₆-eYFP was performed as previously
12 published.²⁹ The concentration of His₆-eYFP was determined by BCA protein assay and
13 measured absorbance at 562 nm.
14
15
16
17
18

19
20 CD spectra were recorded using AVIV and Applied Photophysics Chirascan CD
21 spectrophotometers at 25 °C with a time constant of 5 s and a step resolution of 1 nm in a 1mm
22 quartz cell. CD data are given as mean of residual molar ellipticities ($\text{deg cm}^2 \text{ dmol}^{-1}$). The
23 spectra are the result of 2-4 repeats. All measured solutions contained a final concentration of 4
24 μM His₆-eYFP protein in PBS, where the PBS background spectrum was subtracted.
25
26
27
28

29
30 Fluorescence of 100 nM His₆-eYFP ($\lambda_{\text{ex}} = 513 \text{ nm}$, $\lambda_{\text{em}} = 524 \text{ nm}$) and polymer-protein
31 conjugates was investigated with a PerkinElmer LS55 fluorescence spectrometer (Waltham,
32 Massachusetts, USA) at ambient temperature. Fluorescence of 60 nM RHB-His₆ alone ($\lambda_{\text{ex}} = 554$
33 nm, $\lambda_{\text{em}} = 585 \text{ nm}$) and in complex with NTA- Cu^{2+} , trisNTA- Cu^{2+} and PNT4- Cu^{2+} was measured
34 similarly.
35
36
37
38
39
40
41
42

43 **Binding ability and affinity of His₆-eYFP to PNTn-Me²⁺ copolymers.** Binding stoichiometry
44 and dissociation constant (K_D) were determined by ITC. ITC was carried out using a VP-ITC
45 microcalorimeter from MicroCal. Interaction constants characterizing the PNTn-Me²⁺
46 copolymers and His₆-eYFP were determined by direct titration of His₆-eYFP into polymer
47 solutions in PBS pH 7.4 at 25°C. The concentration of His₆-eYFP and trisNTA on PNTn was 70
48 μM and 6 μM , respectively. During analysis the solution in the sample cell was stirred at 300
49
50
51
52
53
54
55
56
57
58
59
60

1
2
3 rpm. The volume of the sample cell and syringe were 1.4 mL and 295 μ L, respectively. Small
4
5 aliquots of His₆-eYFP (typically 10 μ L) were added into the stirring solution over 240 s to allow
6
7 complete equilibration. The first injection was set to a volume of 1 μ L to avoid air in the syringe
8
9 and ignored for data analysis. Exothermic heat pulse (upper panel, Figure S1) that corresponds
10
11 to an injection of 10 μ L of 70 μ M His₆-eYFP to 1.4 mL of 6 μ M trisNTA functional group on
12
13 copolymers was recorded as a function of time. The data were analyzed using the Origin
14
15 software package supplied by MicroCal and fitted by standard single-site binding model (lower
16
17 panel, Figure S1). The stoichiometry value is equal to the value of the molar ratio for which the
18
19 slope of the plot in lower panel is steepest. The slope of the plot at this point gives the value of
20
21 the reciprocal of the dissociation constant.
22
23
24
25

26
27 **Stability and pH-triggered dissociation of PNTn-Me²⁺-His₆-eYFP conjugates.** FPLC was used
28
29 for the analysis of the stability and the pH responsiveness of PNTn-Me²⁺-His₆-eYFP conjugates.
30
31 250 μ M His₆-eYFP was incubated with a metal cation-coordinated PNTn in PBS with a molar
32
33 ratio of 1 : 2 for His₆-eYFP : trisNTA. The solution (500 μ L) was loaded onto a Superdex 200
34
35 10/300 GL (Akta Prime system, Amersham Biosciences, measuring @ 513 nm), and eluted with
36
37 a PBS mobile phase. For the investigation of pH responsiveness, the column was equilibrated
38
39 with PBS solution at pH 5.0 or 6.0. The sample was prepared in the same way as previously
40
41 described, loaded onto the column and eluted with PBS solution at pH 5.0 or 6.0. The data were
42
43 analyzed by Fityk software to calculate the integral area of the individual peaks.
44
45
46
47

48 **Structure of PNTn-Me²⁺-His₆-eYFP conjugates.** The size of PNTn-Me²⁺-His₆-eYFP
49
50 conjugates were investigated by dynamic light scattering (DLS) with a Zetasizer Nano ZSP
51
52 (Malvern Instruments Ltd., UK) at 25 °C in PBS. The data were fit based on number distribution.
53
54 The concentration of His₆-eYFP was 20 μ M and 800 μ L of solution was used for measurements.
55
56
57
58
59
60

1
2
3 The negatively stained image of PNT4-Zn²⁺-His₆-eYFP conjugates (0.1 mg/mL, 5 μL) stained
4
5 with 2% uranyl acetate was performed on a transmission electron microscope (Philips CM100) at
6
7 an acceleration voltage of 80 kV. The size of the conjugates was analyzed using ImageJ
8
9 software.
10

11
12 **Cell culture.** HeLa cells or U87 glioblastoma cells were maintained at 37 °C in a 5% CO₂
13
14 humidified atmosphere and were grown in DMEM with 10% FBS, 100 units/mL penicillin, 100
15
16 μg/mL streptomycin and 2 mM L-glutamine.
17
18

19
20 **Cell viability.** Cytotoxicity testing was performed using the PromegaCellTiter 96 AQueous Non-
21
22 Radioactive Cell Proliferation (MTS) assay (Promega, USA) to determine the number of viable
23
24 cells in culture. HeLa and U87 cells were seeded in a 96-well plate the night before experiments
25
26 at 0.5×10^4 and 1×10^4 cells/well in 100 μl, respectively. The day of the experiment, samples
27
28 (10μL) containing different amount of PNT4-Me²⁺ (0-375 μg/mL), were added to the cells.
29
30 Twenty-four hours later, 20 μL of MTS solution were added to each well and incubated for 3h at
31
32 37 °C. Cell viability was calculated by measuring the absorbance at 490 nm using a 96-well plate
33
34 reader and plotted relative to untreated cells that were grown the same day in the same plate and
35
36 assays were performed in triplicate.
37
38
39
40
41
42

43 RESULTS AND DISCUSSION

44
45 **Binding stoichiometry of His₆-eYFP to PNTn coordinated with different metal cations.** PNT
46
47 copolymers were previously synthesized and the average distance between trisNTA binding sites
48
49 of PNT1, PNT2, PNT4, and PNT7 of 31.5 nm, 13.2 nm, 5.2 nm and 4.3 nm, were theoretically
50
51 calculated, assuming an idealized linear polymer chain, by dividing the length of the polymer
52
53 chain by the corresponding metal content. These calculations resulted in an average number of 2,
54
55
56
57
58
59
60

1
2
3 4, 7 and 9 trisNTA per polymer, respectively (Table S1).²⁰ Here we are interested to modulate
4 the binding affinity of His-tagged proteins to these polymer chains decorated with tris-NTA
5 groups, and in this respect, we selected three different metal cations, Cu^{2+} , Zn^{2+} , or Fe^{3+} . The
6 binding stoichiometry of His₆-eYFP to the PNT-Meⁿ⁺ was assessed by ITC in order to calculate
7 the dependence of the metal and of the distance between trisNTA sites on binding stoichiometry
8 (Figure 2, S1). His₆-eYFP coordinated the Cu^{2+} or Zn^{2+} metals on PNTn copolymers with a
9 maximum binding stoichiometry approaching 0.9:1 or 0.85:1, respectively, when the average
10 distance between trisNTA binding sites was larger than the size of His₆-eYFP and steric
11 hindrance did not block efficient binding. However, even though PNT7 has a higher content of
12 trisNTA-Me²⁺ sites, a lower binding stoichiometry was observed (0.55 and 0.53 His₆-eYFP to
13 trisNTA-Cu²⁺ and trisNTA-Zn²⁺ sites) due to steric hindrance, resulting from the coil
14 conformation of the polymer in solution. In the case of PNTn containing trisNTA-Fe³⁺, no
15 coordination of His₆-eYFP was observed by ITC even when a high concentration of His₆-eYFP
16 (180 μM) was added (data not shown).
17
18
19
20
21
22
23
24
25
26
27
28
29
30
31
32
33
34
35
36
37
38
39
40
41
42
43
44
45
46
47
48
49
50
51
52
53
54
55
56
57
58
59
60

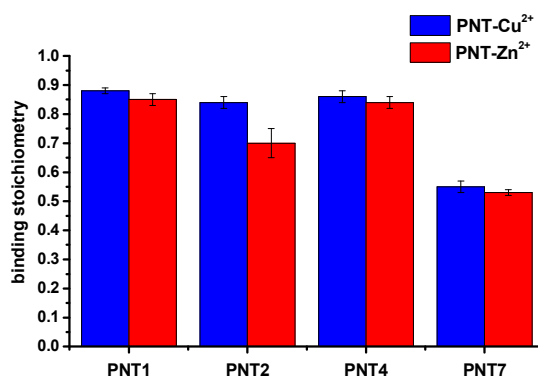


Figure 2. Binding stoichiometry between trisNTA-Me²⁺ in PNTn and His₆-eYFP.

1
2
3 **Binding affinity of His₆-eYFP to PNTn-Me²⁺ copolymers.** In addition to calculating the
4 binding stoichiometry, the binding affinity of His₆-eYFP to PNTn containing either Cu²⁺ or Zn²⁺
5 was compared where the K_D value was normalized per NTA functional group per polymer chain
6 to allow for comparison between the polymers containing different average number of binding
7 sites. Similar to PNTn-Cu²⁺ (0.09-0.39 μ M), K_D values for PNTn-Zn²⁺-His₆-eYFP depended on
8 the average distance between trisNTA binding sites. When the distance was decreased from 31.5
9 nm to 4.3 nm (PNT1-Zn²⁺-His₆-eYFP and PNT7-Zn²⁺-His₆-eYFP, respectively), the K_D values
10 decreased from $1.35 \pm 0.12 \mu$ M to $0.46 \pm 0.06 \mu$ M. It is known that numerous factors play a role
11 in the binding strength of a metal to its coordination pocket including size, charge, protein
12 oligomerization and other stabilizing or destabilizing interactions.³⁰⁻³³ For example, increasing
13 the number of binding sites could decrease the K_D of a small molecule due to a decreased rate of
14 dissociation. On the contrary if the size of proteins is larger than the mean distance between
15 trisNTA-Meⁿ⁺ sites, the binding affinity is decreased even if an increased number of coordination
16 is present due to steric hindrance and charge repulsion of the protein.²⁰ However, increasing the
17 number of trisNTA-Me²⁺ per polymer, effectively decreasing their separation, stabilized the
18 conjugate. While many factors play a role in affinity, this decrease of K_D supports the previous
19 findings that a decrease of enthalpy was seen upon binding of PNT4 compared to PNT1
20 copolymers indicating an increase in hydrogen bond formation from inter-protein interactions.³⁰⁻
21
22
23
24
25
26
27
28
29
30
31
32
33
34
35
36
37
38
39
40
41
42
43
44
45
46 ³³ This led to a binding affinity dependency of PNTn-Me²⁺-His₆-eYFP based on a combined
47 effect between the coordination strength of the metal and the amount of inter-protein
48 interactions, which overcomes the coil-hindrance (Figure 3).
49
50
51
52
53
54
55
56
57
58
59
60

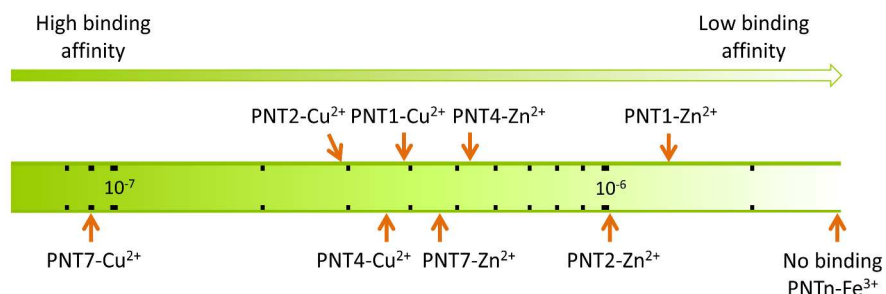


Figure 3. K_D (M) for the binding between PNTn-Cu²⁺/Zn²⁺/Fe³⁺ and His₆-eYFP at pH = 7.4.

The binding affinity of His-tagged proteins is dependent on the strength of coordination with the metal where $\text{Cu}^{2+} > \text{Ni}^{2+} > \text{Zn}^{2+} > \text{Fe}^{3+}$.³⁴ Therefore, Zn²⁺ is rarely used for NTA conventional applications, such as purification of proteins, due to its poor binding affinity ($\log_{10}K = 3.25 \text{ M}^{-1}$).³⁵ Even with the increased binding created by using trisNTA instead of NTA or bisNTA, it is apparent that when inter-protein interactions are not present, as is the case for PNT1, the binding affinity with Zn²⁺ is still much weaker than its Cu²⁺ equivalent. By increasing the inter-protein interactions as a result of an increased number of accessible trisNTA coordination pockets, the binding affinity increases due to stabilization of the conjugates. However, for PNT7 the steric hindrance leads to a decrease in binding stoichiometry as described above. Introducing inter-protein interactions leads to more stable Zn²⁺ conjugates, which makes them suitable for further applications (Figure 3). This strategy is seen in nature to stabilize self-assembled structures by inter-protein interactions.²⁶⁻²⁸

Physical characteristics of PNTn-Me²⁺-His₆-eYFP conjugates and protein stability. The size of PNTn-Me²⁺-His₆-eYFP conjugates was characterized by DLS. PNT1-Cu²⁺/Zn²⁺ and PNT4-Cu²⁺/Zn²⁺ were chosen as representative polymers for further investigations including size measurements and stabilities in various pHs. Even though PNT1 has an average number of 2 trisNTA-Me²⁺ binding sites per polymer, in order to compare a multiple protein system to the

1
2
3 classical one protein per PNT1, a 2 : 1 ratio of trisNTA-Me²⁺ to His₆-eYFP was chosen. Also,
4 since the binding studies showed a stoichiometry < 1 for PNTn polymers to the average number
5 of binding sites, this means each polymer solution has a mixture of polymers containing an
6 average number of accessible binding sites less than the theoretical value (2 for PNT1, and 7 for
7 PNT4). Therefore, this 2 : 1 ratio was used for both PNTn to keep the number of proteins
8 proportional on each polymer chain. For this molar ratio, there are an average of 3 or 4 His₆-
9 eYFPs per polymer chain for PNT4, and an average of one His₆-eYFP per polymer chain for
10 PNT1. In addition, due to the excess of trisNTA-Me²⁺ compared to His₆-eYFP, no free proteins
11 are expected.
12
13
14
15
16
17
18
19
20
21
22
23

24 In order to directly measure the size shift of the tertiary structure of polymer chains in solution
25 due to the binding of proteins, dynamic light scattering was performed. The hydrodynamic
26 diameter (D_H) of His₆-eYFP was determined to be 5.0 ± 0.9 nm. The D_H of PNT1-Zn²⁺ was $8.1 \pm$
27 2.5 nm and when coordinated with His₆-YFP increased in size to 9.7 ± 2.4 nm (Figure S3).
28 PNT4-Zn²⁺ was 5.8 ± 1.8 nm (Figure S2) and after binding, the diameter value shifted to $13.1 \pm$
29 2.8 nm, which was similar to PNT4-Cu²⁺-His₆-eYFP (data not shown). The change in size
30 between PNT1-Zn²⁺ and PNT4-Zn²⁺ after binding His₆-eYFP can be explained by the increased
31 average number of proteins per polymer. The DLS data was supported with transmission electron
32 microscopy (TEM), revealing structures with a diameter of 12 ± 3 nm for PNT4-Zn²⁺-His₆-eYFP
33 (Figure S4).
34
35
36
37
38
39
40
41
42
43
44
45
46
47

48 To address the question of whether the conjugation of polymers to proteins causes alterations in
49 their secondary structure, His₆-eYFP was characterized before and after polymer conjugation by
50 CD spectroscopy. The far-UV CD spectra of His₆-eYFP and PNT1/4-Zn²⁺-His₆-eYFP, showed
51
52
53
54
55
56
57
58
59
60

1
2
3 that conjugation did not alter the protein structure (Figure S5), agreeing with the previously
4 published results.^{20,36}
5
6

7
8 **PNTn-Me²⁺-His₆-eYFP stability under varying pHs.** The stability of PNTn-Me²⁺-His₆-eYFP
9 conjugates under various pH's was investigated by FPLC. Each of the protein-polymer
10 conjugates were measured to establish a baseline of the amount of free His₆-eYFP in each and
11 calculated as a percent of intact protein-polymer complex (Figure 4,). PNT1-Cu²⁺-His₆-eYFP
12 showed a lower stability than PNT4-Cu²⁺-His₆-eYFP at pH 7.4 (Figure S6). The difference
13 between PNT1-Zn²⁺-His₆-eYFP and PNT4-Zn²⁺-His₆-eYFP was even more significant with only
14 46.6% of His₆-eYFP remaining bound with PNT1-Zn²⁺ while 80.2% of His₆-eYFP remaining
15 complexed with PNT4-Zn²⁺. Because PNTn-Me²⁺ copolymers are highly negatively-charged,²⁰
16 the potential electrostatic interactions between protein-polymer conjugates and gel filtration
17 media might decrease the stability of conjugates during the FPLC analysis.³⁷⁻³⁹ This was tested
18 by increasing the number of available PNT4-Zn²⁺ from 2 to 10 equivalents compared to His₆-
19 eYFP. Even with a 5 fold increase in potential interaction sites, the % of free protein remained
20 the same suggesting that the phenomena was caused by interaction with the column (Figure S7).
21 The higher stability of PNT4-Me²⁺-His₆-eYFP compared to PNT1-Me²⁺-His₆-eYFP is attributed
22 to inter-protein interactions preventing the disassociation of the complex, in agreement with the
23 binding affinity values. Inter-protein interactions stabilize the protein-polymer conjugates when
24 the number of trisNTA groups is increased (PNT4 compared with PNT1) strengthening the
25 interaction when the metal is not a strong coordination center (Zn²⁺).
26
27
28
29
30
31
32
33
34
35
36
37
38
39
40
41
42
43
44
45
46
47
48
49
50
51
52
53
54
55
56
57
58
59
60

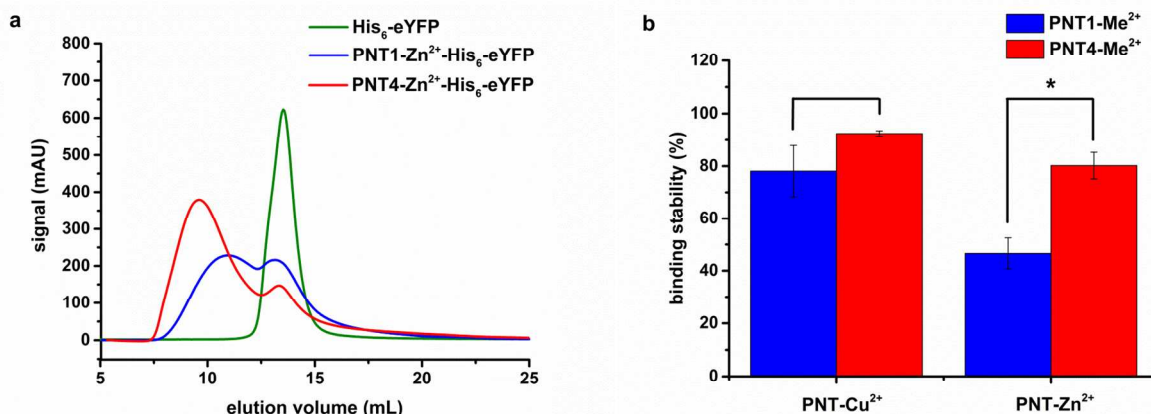


Figure 4. Stability of PNTn-Me²⁺-His₆-eYFP conjugates at pH 7.4. (a) FPLC chromatograms of His₆-eYFP and PNT1/4-Zn²⁺-His₆-eYFP. (b) The percentage of His₆-eYFP bound with PNT1/4-Me²⁺. Stars indicate significance in two-tailed Student's t-test; *P<0.05, n=3.

An attractive property of NTA-Me²⁺-His₆ molecular recognition is pH sensitive binding.¹⁸ However, this property has previously not been proven with trisNTA protein-polymer conjugates. In order to investigate the pH sensitive binding, a model peptide, hexahistidine labeled with Rhodamine B (RHB-His₆) was used to compare the parameters that effect binding stability across various pHs. RHB-His₆ is strongly quenched when bound to Cu²⁺, and more stable than eYFP at lower pH.⁴⁰ The binding of trisNTA-Cu²⁺ to RHB-His₆ resulted in a significant decrease of fluorescent intensity from 570 to 60. The fluorescent intensity remained unchanged at all pH > 3.5 (Figure S8), indicating that the binding between trisNTA-Cu²⁺ and RHB-His₆ is stable at various pHs. PNT4-Cu²⁺-RHB-His₆ exhibited no dissociation with pH > 3.5, suggesting that the presence of polymer does not significantly influence the binding stability. Also, PNT4-Cu²⁺ did not show a significant release of His₆-eYFP when the pH was changed from 7.4 to 6.0, but 52% of the conjugates disassociated at pH 5.0, respectively (Figure 5). As expected, due to the lack of inter-protein interactions, the release of His₆-eYFP was more

1
2
3 pronounced for PNT1-Cu²⁺ at pH values down to 6, ending at pH =5 to a similar fraction of
4 dissociated conjugates (53%). The higher percent of pH-triggered dissociation can be attributed the
5
6 higher K_D at pH 7.4 of PNT4-Cu²⁺-His₆-eYFP ($K_D=0.36 \mu\text{M}$) compared with PNT4-Cu²⁺-RHB-
7
8 His₆ ($K_D=0.13 \mu\text{M}$).²⁰ In contrast with PNTn-Cu²⁺, both PNT1-Zn²⁺ and PNT4-Zn²⁺ exhibited a
9
10 more rapid dissociation. At pH 7.4 PNT1-Zn²⁺ and PNT4-Zn²⁺ dissociated from His₆-eYFP at
11
12 53.4% compared to 19.8% determined by FPLC, respectively. Decreasing the pH to 6.0
13
14 increased the dissociation of His₆-eYFP from PNT1-Zn²⁺ and PNT4-Zn²⁺ to 92% and 76%,
15
16 respectively, with both conjugates being completely unbound by pH 5.0 (Figure 5 a, b). The
17
18 higher dissociation of PNTn-Zn²⁺-His₆-eYFP compared with PNTn-Cu²⁺-His₆-eYFP at lower pH
19
20 was expected, due to the higher K_D values (0.46-1.35 μM , 0.09-0.39 μM , respectively). The
21
22 trisNTA-Cu²⁺ binding sites on PNTn have stronger interaction with His₆-eYFP compared with
23
24 protons ($K_D \approx 1 \mu\text{M}$),^{18,41} therefore it is difficult to be protonated to induce the dissociation of the
25
26 proteins. However, the affinity of trisNTA-Zn²⁺ on PNTn to His₆-eYFP is comparable to that of
27
28 protons, resulting in direct competition between protonation and coordination of the His₆-eYFP.
29
30 This led to PNTn-Zn²⁺-His₆-eYFP having a higher amount of pH-triggered release than PNT-Cu²⁺-
31
32 His₆-eYFP. Furthermore, the reversibility of pH dependent binding of PNT4-Zn²⁺-His₆-eYFP was
33
34 investigated due to its higher pH binding dependence. A solution of PNT4-Zn²⁺-His₆-eYFP was
35
36 formed in pH 7.4 and tested for stability, the pH was then decreased to 5.0 and dissociation was
37
38 observed. However, when the pH was increased back to pH 7.4 almost complete reformation of
39
40 all protein complexes was observed (Figure 5c).
41
42
43
44
45
46
47
48
49
50
51
52
53
54
55
56
57
58
59
60

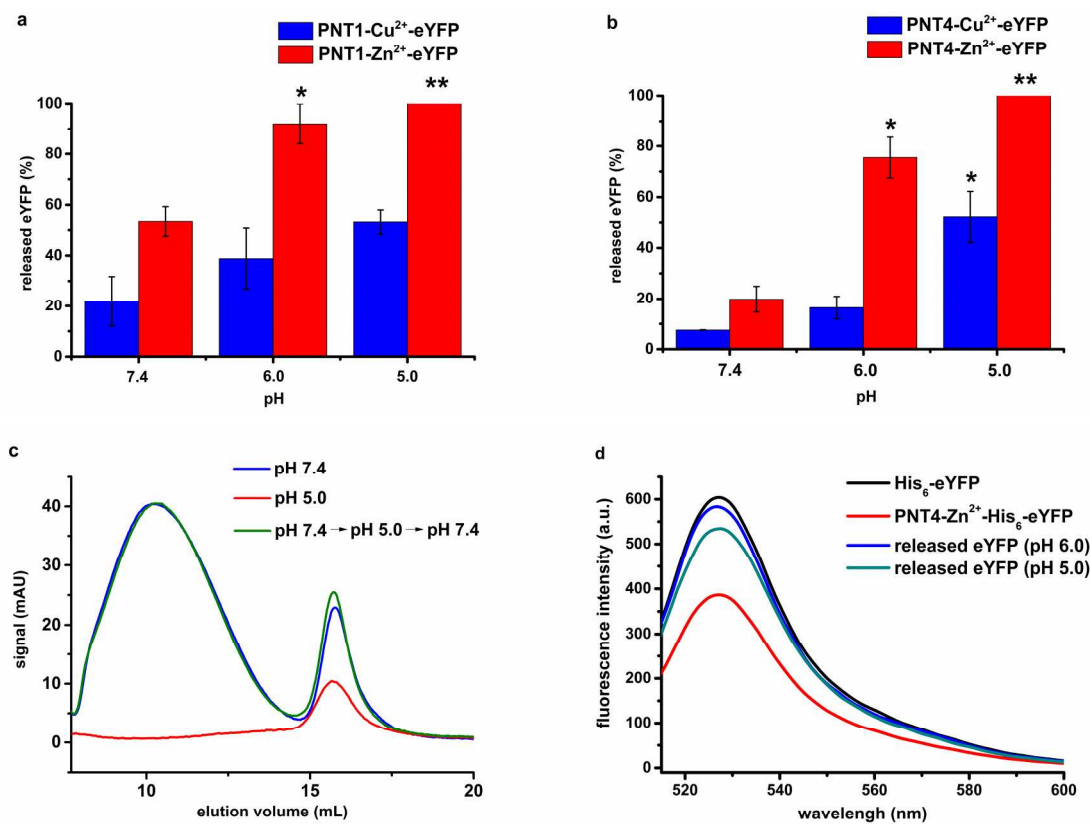


Figure 5. Release of His₆-eYFP from PNT1-Me²⁺ (a) and PNT4-Me²⁺ (b) at different pH values.

All statistics were analyzed by comparing samples to their respective protein-polymer conjugate at pH 7.4. Stars indicate significance compared to the equivalent protein polymer conjugate at pH 7.4 in a two-tailed Student's t-test; *P<0.05, **P<0.005. (c) Reversibility of pH dependent

binding between PNT4-Zn²⁺ and His₆-eYFP analyzed by FPLC. (d) The fluorescence emission spectra of His₆-eYFP and PNT4-Zn²⁺-His₆-eYFP before and after release in acidic conditions.

While reactions were run in acidic conditions, all samples were analyzed at pH 7.4 in PBS.

To address the question of whether the reversible binding of PNTn copolymers to His₆-eYFP influence its fluorescent property, His₆-eYFP was characterized by fluorescence spectroscopy before and after polymer conjugation (Figure 5d). When His₆-eYFP was conjugated with PNT4-

1
2
3 Zn^{2+} , a decrease in fluorescence intensity was observed due to the chelation with Zn^{2+} . After
4
5 dissociation from PNT4- Zn^{2+} in acidic conditions (pH = 5.0 or 6.0), the released His₆-eYFP was
6
7 collected and then buffered back to pH 7.4, the fluorescence of His₆-eYFP recovered almost to
8
9 its original value. The slight decrease of fluorescence intensity was due to short-term exposure to
10
11 acidic condition which corresponds to literature precedence.⁴² In addition, the second structure of
12
13 dissociated His₆-eYFP after buffering back pH 7.4 was evaluated by CD spectroscopy. No
14
15 obvious change of the spectrum was observed, suggesting His₆-eYFP was kept intact during the
16
17 pH-triggered dissociation (Figure S9). Therefore, PNTn copolymers are able to bind His₆-eYFP
18
19 at physiological pH and release the bound protein in acidic conditions without influencing the
20
21 structure and properties.
22
23
24
25

26
27 **Cytotoxicity evaluation of PNT4-Meⁿ⁺ copolymers.** The cytotoxicity of PNT4-Meⁿ⁺
28
29 copolymers was evaluated on U87 and HeLa cells by using the MTS assay (Figure 6). PNT4
30
31 copolymer showed low toxicity in all range of concentrations tested in both cell lines. The
32
33 coordination of PNT4 with Zn^{2+} did not induce toxicity in contrast to PNT4 coordinated with
34
35 Cu^{2+} or Ni^{2+} that showed toxicity with increasing concentrations (Figure S10). trisNTA
36
37 coordinated with Cu^{2+} , Ni^{2+} , Zn^{2+} was tested as a control and showed slightly higher toxicity
38
39 compared to equivalent copolymer samples (Figure S10). Repeat administrations of Cu^{2+} or Ni^{2+}
40
41 can accumulate in the liver, kidney, and spleen, leading to organ damage after the complex has
42
43 dissociated and the metal released.⁴³⁻⁴⁶ Therefore in terms of its low toxicity, a protein-polymer
44
45 conjugate comprised of PNT4 and Zn^{2+} would be suitable for further in vitro studies.
46
47
48
49
50
51
52
53
54
55
56
57
58
59
60

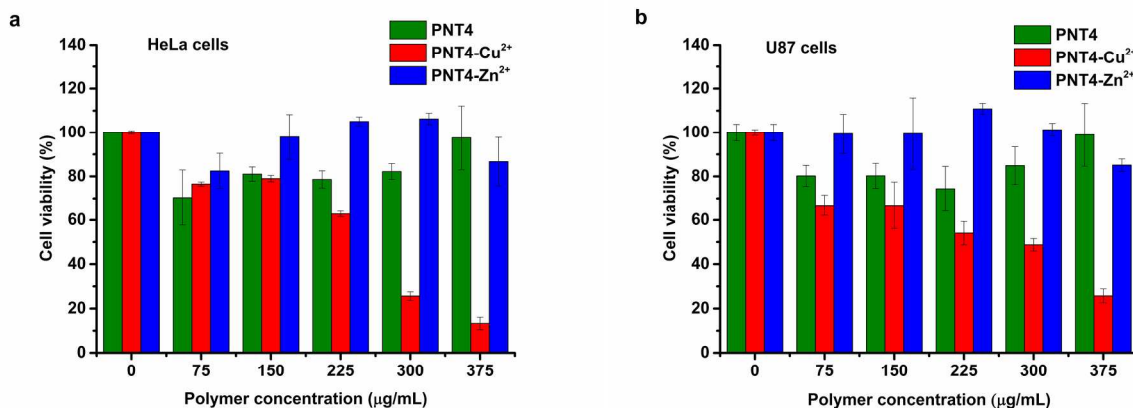


Figure 6. Toxicity evaluation of PNT4-Meⁿ⁺ copolymers on HeLa (a) and U87 (b) cells using MTS assay where zero polymer concentration refers to the addition of PBS to the cells. Errors bars represent the standard deviation (n=3).

CONCLUSION

An efficient method to site-specifically and reversibly bind multiple proteins per polymer chain using trisNTA-Me²⁺-His₆ molecular recognition was designed. His₆-eYFP was used as a model protein for binding PNT-Meⁿ⁺ copolymers. It was demonstrated that the nature of the Meⁿ⁺ and the number of metal binding pockets of trisNTA enable great selectivity for the binding affinity. This led to control of the stability and pH triggered release of the protein from the polymer by modulating inter-protein interactions. After complete release of His₆-eYFP from PNT-Me²⁺ copolymers at selective pH, the return of fluorescence suggested that the protein was intact and maintained its properties. In addition, the toxicity problem of trisNTA-Meⁿ⁺ and its derivatives, has been improved by using Zn²⁺, which still maintained the binding with His₆-eYFP due to controllable inter-protein interactions.

The presented system advances the field from covalent single protein-polymer conjugates to non-covalent multiple protein-polymer conjugates that can be readily formed and dissociated

1
2
3 dependent on pH, and serves as a platform for the combination of various active agents into one
4
5 nanosystem to potentially fulfill multiple tasks such as therapy and diagnosis in a combined
6
7
8 manner.
9

10 **ASSOCIATED CONTENT**

13 **Supporting information**

14
15
16
17 Characterization of protein-polymer conjugates, additional cell toxicity data, fluorescent spectra
18
19 of trisNTA-Cu²⁺-RHB-His₆ in various pH and CD spectra of His₆-eYFP. This material is
20
21 available free of charge via the Internet at <http://pubs.acs.org>.
22
23
24

25 **AUTHOR INFORMATION**

28 **Corresponding Authors**

29
30
31 * tel: +41 (0)61 267 38 39; fax: +41 (0)61 267 38 55; cornelia.palivan@unibas.ch
32
33

34
35 * tel: +41 (0)61 267 38 02; fax: +41 (0)61 267 38 55; wolfgang.meier@unibas.ch
36
37

38 **Notes**

39
40 The authors declare no competing financial interest.
41
42

43 **ACKNOWLEDGMENT**

44
45
46 We thank Swiss National Science Foundation and University of Basel for financial support. J. L.
47
48 thanks China Scholarship Council for supporting the fee to study abroad. We thank Biozentrum
49
50 Biophysics Facility Basel for the use of their ITC instrument. J. L. thanks Mariana Spulber from
51
52 University of Basel for extensive discussions.
53
54
55

56 **REFERENCES**

- 1
2
3 (1) Leader, B.; Baca, Q. J.; Golan, D. E. Protein Therapeutics: a Summary and
4
5 Pharmacological Classification. *Nat. Rev. Drug Discov.* **2008**, *7*, 21-39.
6
7
- 8
9 (2) Frokjaer, S.; Otzen, D. E. Protein Drug Stability: a Formulation Challenge. *Nat. Rev.*
10
11 *Drug Discov.* **2005**, *4*, 298-306.
12
13
- 14 (3) De Groot, A. S.; Scott, D. W. Immunogenicity of Protein Therapeutics. *Trends Immunol.*
15
16 **2007**, *28*, 482-490.
17
18
- 19
20 (4) Duncan, R. Polymer Conjugates as Anticancer Nanomedicines. *Nat. Rev. Cancer.* **2006**,
21
22 *6*, 688-701.
23
24
- 25 (5) Knop, K.; Hoogenboom, R.; Fischer, D.; Schubert, U. S. Poly(ethylene glycol) in Drug
26
27 Delivery: Pros and Cons as Well as Potential Alternatives. *Angew. Chem., Int. Ed.* **2010**, *49*,
28
29 6288-6308.
30
31
- 32
33 (6) Kolate, A.; Baradia, D.; Patil, S.; Vhora, I.; Kore, G.; Misra, A. PEG - aVersatile
34
35 Conjugating Ligand for Drugs and Drug Delivery Systems. *J. Control. Release* **2014**, *192*, 67-81.
36
37
- 38
39 (7) Pelegri-O'Day, E. M.; Lin, E.-W.; Maynard, H. D. Therapeutic Protein–Polymer
40
41 Conjugates: Advancing Beyond PEGylation. *J. Am. Chem. Soc.* **2014**, *136*, 14323-14332.
42
43
- 44 (8) Harris, J. M.; Chess, R. B. Effect of Pegylation on Pharmaceuticals. *Nat. Rev. Drug*
45
46 *Discov.* **2003**, *2*, 214-221.
47
48
- 49
50 (9) Gauthier, M. A.; Klok, H.-A. Polymer-Protein Conjugates: an Enzymatic Activity
51
52 Perspective. *Polym. Chem.* **2010**, *1*, 1352-1373.
53
54
55
56
57
58
59
60

- 1
2
3 (10) Secundo, F. Conformational Changes of Enzymes upon Immobilisation. *Chem. Soc. Rev.*
4
5 **2013**, *42*, 6250-6261.
6
7
8
9 (11) Filpula, D.; Zhao, H. Releasable PEGylation of Proteins with Customized Linkers. *Adv.*
10
11 *Drug Deliv. Rev.* **2008**, *60*, 29-49.
12
13
14 (12) Tao, L.; Liu, J.; Xu, J.; Davis, T. P. Bio-Reversible polyPEGylation. *Chem. Commun.*
15
16 **2009**, 6560-6562.
17
18
19
20 (13) Gong, Y.; Leroux, J.-C.; Gauthier, M. A. Releasable Conjugation of Polymers to
21
22 Proteins. *Bioconjugate Chem.* **2015**, DOI: 10.1021/bc500611k.
23
24
25
26 (14) Kulkarni, S.; Schilli, C.; Grin, B.; Müller, A. H. E.; Hoffman, A. S.; Stayton, P. S.
27
28 Controlling the Aggregation of Conjugates of Streptavidin with Smart Block Copolymers
29
30 Prepared via the RAFT Copolymerization Technique. *Biomacromolecules* **2006**, *7*, 2736–2741.
31
32
33
34 (15) Chen, J.; Zhao, M.; Feng, F.; Sizovs, A.; Wang, J. Tunable Thioesters as “Reduction”
35
36 Responsive Functionality for Traceless Reversible Protein PEGylation. *J. Am. Chem. Soc.* **2013**,
37
38 *135*, 10938-10941.
39
40
41
42 (16) Kim, T. H.; Swierczewska, M.; Oh, Y.; Kim, A.; Jo, D. G.; Park, J. H.; Byun, Y.;
43
44 Sadegh-Nasseri, S.; Pomper, M. G.; Lee, K. C. **et al.** Mix to Validate: a Facile, Reversible
45
46 PEGylation for Fast Screening of Potential Therapeutic Proteins In Vivo. *Angew. Chem., Int. Ed.*
47
48 **2013**, *52*, 6880-6884.
49
50
51
52 (17) Nguyen, T. H.; Kim, S.-H.; Decker, C. G.; Wong, D. Y.; Loo, J. A.; Maynard, H. D. A
53
54 Heparin-Mimicking Polymer Conjugate Stabilizes Basic Fibroblast Growth Factor. *Nat Chem.*
55
56 **2013**, *5*, 221-227.
57
58
59
60

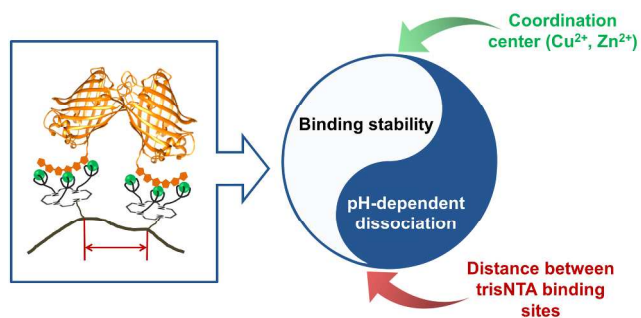
- 1
2
3
4
5
6
7
8
9
10
11
12
13
14
15
16
17
18
19
20
21
22
23
24
25
26
27
28
29
30
31
32
33
34
35
36
37
38
39
40
41
42
43
44
45
46
47
48
49
50
51
52
53
54
55
56
57
58
59
60
- (18) June, R. K.; Gogoi, K.; Eguchi, A.; Cui, X.-S.; Dowdy, S. F. Synthesis of a pH-Sensitive Nitrilotriacetic Linker to Peptide Transduction Domains to Enable Intracellular Delivery of Histidine Imidazole Ring-Containing Macromolecules. *J. Am. Chem. Soc.* **2010**, *132*, 10680-10682.
- (19) André, T.; Reichel, A.; Wiesmüller, K.-H.; Tampé, R.; Piehler, J.; Brock, R. Selectivity of Competitive Multivalent Interactions at Interfaces. *ChemBioChem* **2009**, *10*, 1878-1887.
- (20) Liu, J.; Spulber, M.; Wu, D.; Talom, R. M.; Palivan, C. G.; Meier, W. Poly(N-Isopropylacrylamide-co-Tris-Nitrilotriacetic Acid Acrylamide) for a Combined Study of Molecular Recognition and Spatial Constraints in Protein Binding and Interactions. *J. Am. Chem. Soc.* **2014**, *136*, 12607-12614.
- (21) Lata, S.; Reichel, A.; Brock, R.; Tampé, R.; Piehler, J. High-Affinity Adaptors for Switchable Recognition of Histidine-Tagged Proteins. *J. Am. Chem. Soc.* **2005**, *127*, 10205-10215.
- (22) Grunwald, C.; Schulze, K.; Reichel, A.; Weiss, V.; Blaas, D.; Piehler, J.; Wiesmüller, K.; Tampé, R. In Situ Assembly of Macromolecular Complexes Triggered by Light. *Proc. Natl. Acad. Sci. U.S.A.* **2010**, *107*, 6146.
- (23) Huang, Z.; Hwang, P.; Watson, D. S.; Cao, L.; Szoka, F. C. Tris-Nitrilotriacetic Acids of Subnanomolar Affinity Toward Hexahistidine Tagged Molecules. *Bioconjugate Chem.* **2009**, *20*, 1667-1672.

- 1
2
3 (24) Nehring, R.; Palivan, C. G.; Casse, O.; Tanner, P.; Tu xen, J.; Meier, W. Amphiphilic
4 Diblock Copolymers for Molecular Recognition: Metal-Nitrilotriacetic Acid Functionalized
5 Vesicles. *Langmuir* **2008**, *25*, 1122-1130.
6
7
8
9
10
11 (25) Broyer, R. M.; Grover, G. N.; Maynard, H. D. Emerging Synthetic Approaches for
12 Protein-Polymer Conjugations. *Chem. Commun.* **2011**, *47*, 2212-2226.
13
14
15
16
17 (26) Bolanos-Garcia, V. M.; Wu, Q.; Ochi, T.; Chirgadze, D. Y.; Sibanda, B. L.; Blundell, T.
18 L. Spatial and Temporal Organization of Multi-Protein Assemblies: Achieving Sensitive Control
19 in Information-Rich Cell-Regulatory Systems. *Phil. Trans. R. Soc. A* **2012**, *370*, 3023-3039.
20
21
22
23
24
25 (27) Nussinov, R.; Jang, H. Dynamic Multiprotein Assemblies Shape the Spatial Structure of
26 Cell Signaling. *Prog. Biophys. Mol. Biol.* **2014**, *116*, 158-164.
27
28
29
30
31 (28) Saka, S. K.; Honigmann, A.; Eggeling, C.; Hell, S. W.; Lang, T.; Rizzoli, S. O. Multi-
32 Protein Assemblies Underlie the Mesoscale Organization of the Plasma Membrane. *Nat.*
33 *Commun.* **2014**, *5*, 4059.
34
35
36
37
38 (29) Bruns N.; Pustelny K.; Bergeron L.; Whiehead T.; Ckark D. Mechanical Nanosensor
39 Based on FRET Within a Thermosome: Damage-Reporting Polymeric Materials. *Angew. Chem.,*
40 *Int. Ed.* **2009**, *48*, 5666-5669.
41
42
43
44
45
46 (30) Griffith, B. R.; Allen, B. L.; Rapraeger, A. C.; Kiessling, L. L. A Polymer Scaffold for
47 Protein Oligomerization. *J. Am. Chem. Soc.* **2004**, *126*, 1608-1609.
48
49
50
51
52 (31) Saluja, A.; Kalonia, D. S. Nature and Consequences of Protein-Protein Interactions in
53 High Protein Concentration Solutions. *Int. J. Pharm.* **2008**, *358*, 1-15.
54
55
56
57 (32) Van Rijn, P. Polymer Directed Protein Assemblies. *Polymers* **2013**, *5*, 576-599.
58
59
60

- 1
2
3
4
5
6
7
8
9
10
11
12
13
14
15
16
17
18
19
20
21
22
23
24
25
26
27
28
29
30
31
32
33
34
35
36
37
38
39
40
41
42
43
44
45
46
47
48
49
50
51
52
53
54
55
56
57
58
59
60
- (33) Cairo, W. C.; Gestwicki, E. J.; Kanai, M.; Kiessling, L. L. Control of Multivalent Interactions by Binding Epitope Density. *J. Am. Chem. Soc.* **2002**, *124*, 1615-1619.
- (34) Choe, W.-S.; Clemmitt, R. H.; Chase, H. A.; Middelberg, A. P. J. Comparison of Histidine-Tag Capture Chemistries for Purification Following Chemical Extraction. *J. Chromatogr. A* **2002**, *953*, 111-121.
- (35) Stadlbauer, S. Coordination Chemistry in Molecular Recognition. Ph.D. Dissertation, University of Regensburg, Regensburg, **2009**.
- (36) Xia, Y.; Tanga, S.; Olsen, B. D. Site-Specific Conjugation of RAFT Polymers to Proteins via Expressed Protein Ligation. *Chem. Commun.* **2013**, *49*, 2566-2568.
- (37) Pujar N. S.; Zydney A. L. Electrostatic Effects on Protein Partitioning in Size-Exclusion Chromatography and Membrane Ultrafiltration. *J. Chromatogr. A* **1998**, *796*, 229-238.
- (38) Arakawa T.; Ejima D.; Li T. S.; Philo J. S. The Critical Role of Mobile Phase Composition in Size Exclusion Chromatography of Protein Pharmaceuticlas. *J. Pharm. Sci.* **2009**, *99*, 1674-1692.
- (39) Stulik K.; Pacaova V.; Ticha M. Some Potentialities and Drawbacks of Contemporary Size-Exclusion Chromatography. *J. Biochem. Bioph. Methods* **2003**, *56*, 1-13.
- (40) Lata, S.; Gavutis, M.; Tampé, R.; Piehler, J. Specific and Stable Fluorescence Labeling of Histidine-Tagged Proteins for Dissecting Multi-Protein Complex Formation. *J. Am. Chem. Soc.* **2006**, *128*, 2365-2372.

- 1
2
3 (41) Liu, T.; Ryan, M.; Dahlquist, F. W.; Griffith, O. H. Determination of pKa Values of the
4 Histidine Side Chains of Phosphatidylinositol-Specific Phospholipase C from *Bacillus Cereus* by
5 NMR Spectroscopy and Site-Directed Mutagenesis. *Protein Sci.* **1997**, *6*, 1937-1944.
6
7
8
9
10
11 (42) Anderson, D. E.; Becktel, W. J.; Dahlquist, F. W. pH-Induced Denaturation of Proteins: a
12 Single Salt Bridge Contributes 3-5 kcal/mol to the Free Energy of Folding of T4 Lysozyme.
13 *Biochemistry* **1990**, *29*, 2403-2408.
14
15
16
17
18
19 (43) Turnlund, J. R. Human Whole-Body Copper Metabolism. *Am. J. Clin. Nutr.* **1998**, *67*,
20 960S-964S.
21
22
23
24
25 (44) Pereira, M. C.; Pereira, M. L.; Sousa, J. P. Evaluation of Nickel Toxicity on Liver,
26 Spleen, and Kidney of Mice after Administration of High-Dose Metal Ion. *J. Biomed. Mater.*
27 *Res.* **1998**, *40*, 40-47.
28
29
30
31
32
33 (45) Gupta, S. Cell Therapy to Remove Excess Copper in Wilson's Disease. *Ann. N. Y. Acad.*
34 *Sci.* **2014**, *1315*, 70-80.
35
36
37
38 (46) Guo, H.; Wu, B.; Cui, H.; Peng, X.; Fang, J.; Zuo, Z.; Deng, J.; Wang, X.; Deng, J.; Yin,
39 S. **et al.** NiCl₂-Down-Regulated Antioxidant Enzyme mRNA Expression Causes Oxidative
40 Damage in the Broiler's Kidney. *Biol. Trace Elem. Res.* **2014**, *162*, 288-295.
41
42
43
44
45
46
47
48
49
50
51
52
53
54
55
56
57
58
59
60

Table of Contents Graphic



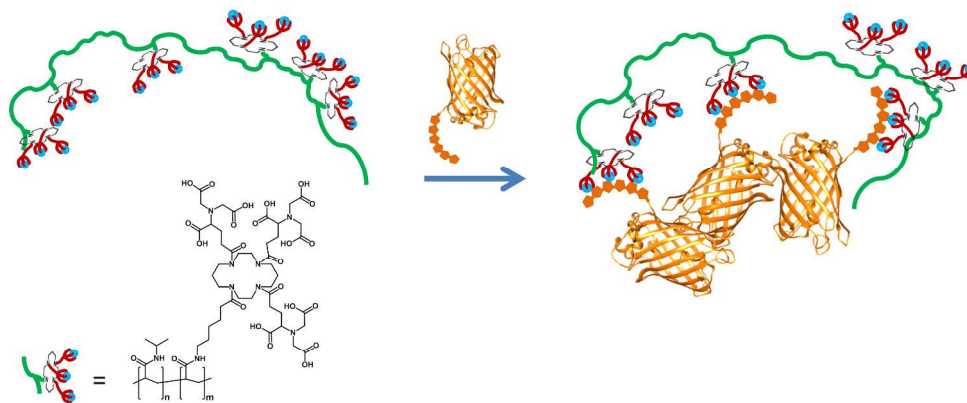


Figure 1. Schematic representation of site-specific conjugation of poly(N-isopropylacrylamide-co-tris-nitrilotriacetic acid acrylamide) polymers (green), which coordinate metals (blue) with His-tagged proteins (orange).

251x114mm (300 x 300 DPI)

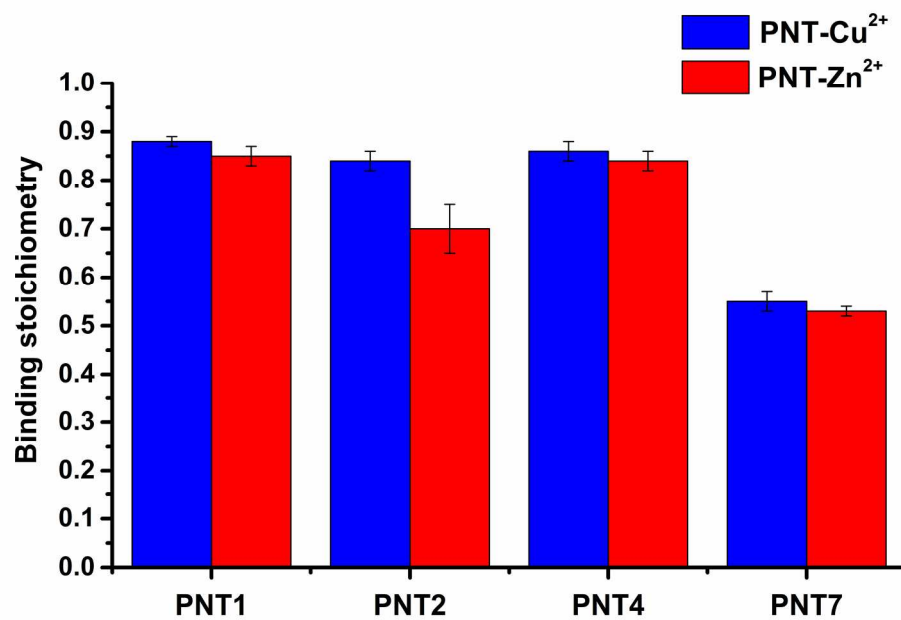


Figure 2. Binding stoichiometry between trisNTA-Me₂⁺ in PNTn and His6-eYFP.
201x140mm (300 x 300 DPI)

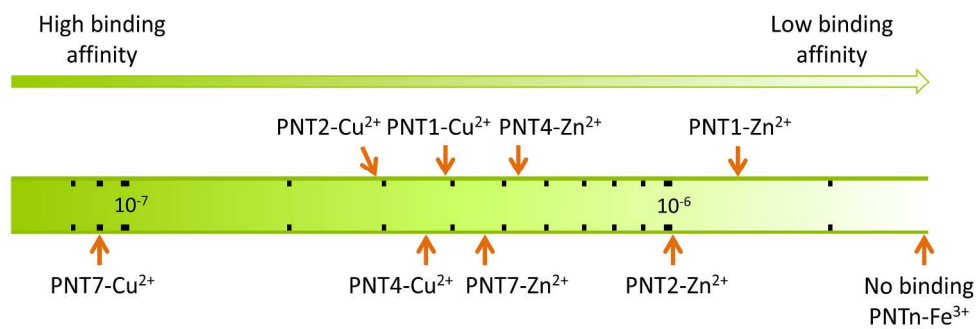


Figure 3. K_D (M) for the binding between PNTn-Cu²⁺/Zn²⁺/Fe³⁺ and His6-eYFP at pH = 7.4.
253x87mm (300 x 300 DPI)

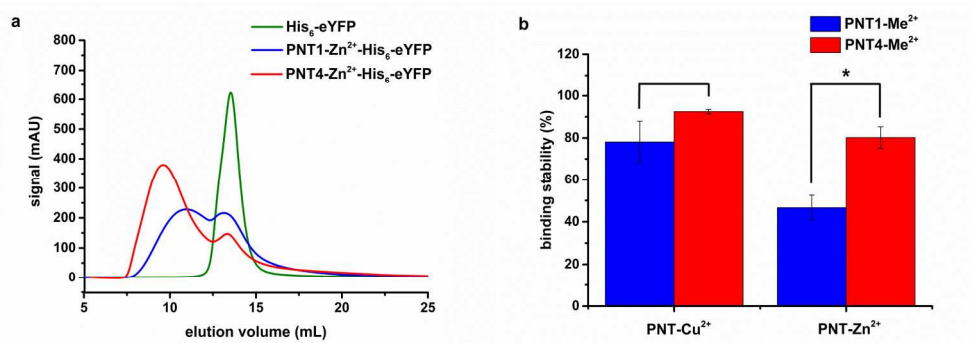


Figure 4. Stability of PNT_n-Me₂⁺-His₆-eYFP conjugates at pH 7.4. (a) FPLC chromatograms of His₆-eYFP and PNT1/4-Zn²⁺-His₆-eYFP. (b) The percentage of His₆-eYFP bound with PNT1/4-Me₂⁺. Stars indicate significance in two-tailed Student's t-test; *P<0.05, n=3.

238x92mm (300 x 300 DPI)

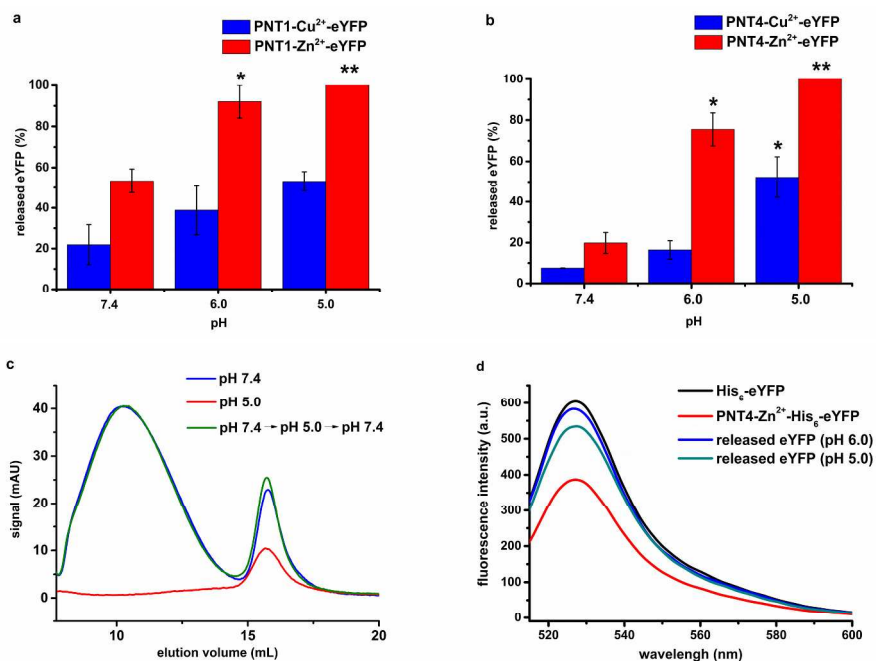


Figure 5. Release of His₆-eYFP from PNT1-Me₂⁺ (a) and PNT4-Me₂⁺ (b) at different pH values. All statistics were analyzed by comparing samples to their respective protein-polymer conjugate at pH 7.4. Stars indicate significance compared to the equivalent protein polymer conjugate at pH 7.4 in a two-tailed Student's t-test;

*P<0.05, **P<0.005. (c) Reversibility of pH dependent binding between PNT4-Zn²⁺ and His₆-eYFP analyzed by FPLC. (d) The fluorescence emission spectra of His₆-eYFP and PNT4-Zn²⁺-His₆-eYFP before and after release in acidic conditions. While reactions were run in acidic conditions, all samples were analyzed at pH 7.4 in PBS.

254x190mm (300 x 300 DPI)

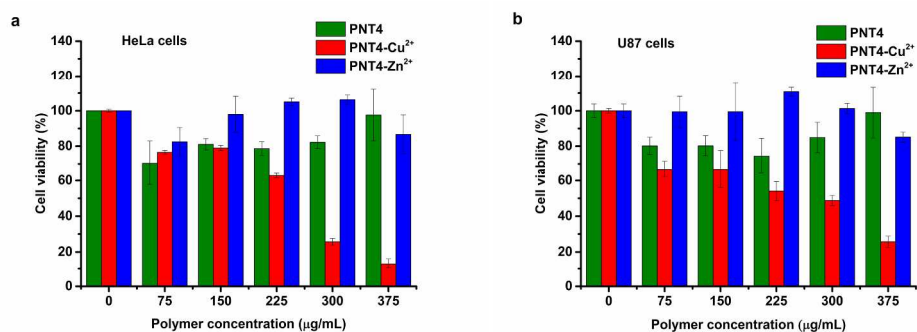
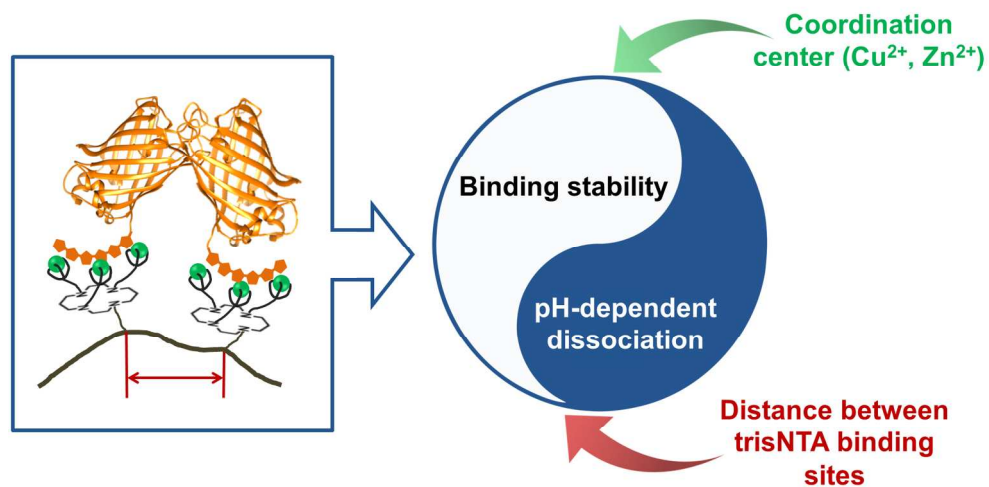


Figure 6. Toxicity evaluation of PNT4-Men⁺ copolymers on HeLa (a) and U87 (b) cells using MTS assay where zero polymer concentration refers to the addition of PBS to the cells. Errors bars represent the standard deviation (n=3).

244x91mm (300 x 300 DPI)



Graphical abstract
325x175mm (150 x 150 DPI)